# A Synchronous/Permanent Magnet Hybrid AC Machine

Xiaogang Luo, *Member, IEEE,* and Thomas A. Lipo, *Fellow, IEEE*

***Abstract*— In this paper, a synchronous/permanent magnet hybrid(SynPM) machine is presented. It is shown that the machine has good power density and efficiency, and that the machine has true field regulation capability. The principle of operation, finite element analysis and simulation of this new machine are investigated in the paper.**

***Index Terms*—Field weakening, hybrid, permanent magnet machine, synchronous machine.**

## I. Introduction

With the advent of power electronics, control technology, and micro-electronics, AC drives are replacing the DC drives in many applications [1], [2]. Meanwhile, extensive efforts have been made on the research and development of electric motors suitable for AC drives applications [1], [3], [4]. Electric motors most widely used in AC drives are induction motors, permanent magnetic brushless DC motors, variable reluctance motors and synchronous reluctance motors [2].

As permanent magnet(PM) materials have improved rapidly for the past two decades, PM machines become a powerful competitor for the motor of choice for AC drives especially for small power ratings due to their high power density and efficiency. The use of PM excitation essentially eliminates the excitation penalty which exists in all other types of electric machines. With the recent development of high coercivity, high residual flux density and high energy product PM material a significantly high air gap flux density can be obtained with proper design, which further increases the power density of PM machines. However, PM materials have the property of low permeability (effectively as low as air) so that regulating the field in a permanent magnet requires large amount of MMF. This feature has greatly limited the use of PM motors in high speed applications where field weakening ability of electric motor is desirable. On the other hand, synchronous machines have very good field regulation capability. This is a result of their relatively small air gap and powerful field winding. However, this benefit is at the cost of excitation loss and slip ring and brushes, which increases the chance of failure and cost of maintenance.

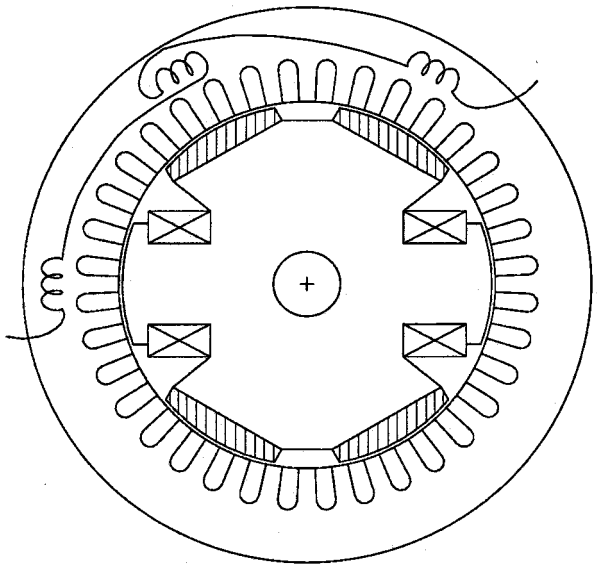

Fig. 1. Structure of SynPM machine.

In this paper, a new electric machine termed the SynPM Hybrid machine is presented. This new machine is a combination of a PM machine and a wound field synchronous machine. It has both PM poles and excitation poles on the rotor, retaining the conventional multi-phase machine stator winding. It has both the features of both PM and synchronous machines. The PM poles provide the air gap with major part of air gap flux. The excitation poles act as the flux regulator to adjust the air gap flux distribution. By proper connection of the stator windings, field weakening/strengthening operation is achieved by picking up the EMF changes caused by the change of flux density under the excitation poles. Although the slip rings and brushes are still present in this kind of electric machine, failure of the brush rigging will not cause as severe a problem as it would for the conventional wound field synchronous machine since the PM poles still produce fair large air gap flux even with the field winding out of service.

## II. Principle of Operation

The structure of the SynPM machine is shown in Fig. 1. The machine has six poles in which 4 of the rotor poles are PM poles and the remaining 2 poles are excitation poles. In general, the operation of this type of machines is quite similar to that of the

Manuscript received July 27, 1998; revised January 26, 1999. This work was supported by the ERC Program of the National Science Foundation under Award Number EEC-9731677.

X. Luo is with the TransDimension International Corporation, Riverside, CA 92507 USA.

T. Lipo is with the Department of Electrical and Computer Engineering University of Wisconsin-Madison, Madison, WI 53706 USA.

Publisher Item Identifier S 0885-8969(00)04524-1.

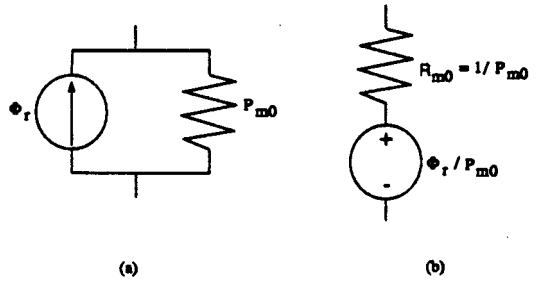


Fig. 2. Equivalent circuit of permanent magnet.

permanent magnet synchronous machine except that this new structure possesses field regulation characteristics.

### A. Ideal Magnetic Circuit Analysis

For easy understanding of tho operation principle, an ideal magnetic circuit analysis is helpful In this analysis, the following points are assumed

1. The iron has infinite permeance.
2. Fringing and leakage fluxes are neglected.
3. Even distribution of flux under a pole.
4. Even distribution of flux in the region between poles.
5. Smooth surfaces on both stator bore and rotor poles.

*1) Permanent Magnet Equivalent Circuit:* A permanent magnet can be represented by a "Norton" equivalent circuit conducting of a flux generator $\Phi_r$ in parallel with an internal leakage permeance $P_{m0}$ [3]. Fig. 2(a) shows the circuit representation. The parameters are calculated by equations (1) and (2):

$$\Phi_r = B_r A_m \tag{1}$$

$$P_{m0} = \frac{\mu_o \mu_{rec} A_m}{l_m} \tag{2}$$

where

$A_m$ the pole area of the magnet,
$l_m$ the magnet length in the direction of magnetization,
$B_r$ the remnant flux density,
$\mu_{rec}$ the relative recoil permeability.

According to Thevenin's Theorem, the equivalent circuit can be changed to the form of an MMF source $F_{pm}$ in series with an internal magnetic reluctance $R_{m0}$, as shown in Fig. 2(b), where

$$F_{pm} = \frac{\Phi_r}{P_{m0}} \tag{3}$$

$$R_{m^O} = \frac{1}{P_{m0}} \tag{4}$$

Having obtained the equivalent circuit of permanent magnet, a magnetic circuit model of SynPM machine can be constructed and is shown in Fig. 3. The circuit model has two rings, representing stator core and rotor core, twelve magnetic reluctances, and six MMF sources. In this model $R_g$ is the air gap reluctance of the excitation poles and is calculated by

$$R_g = \frac{l_g}{\mu_0 A_g} \tag{5}$$

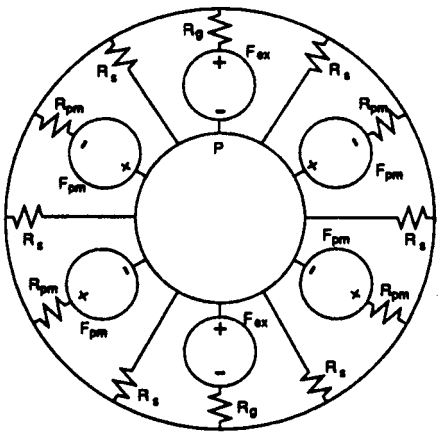


Fig. 3. Magnetic circuit model of 6 pole SynPM machines.

where $l_g$ is the length of air gap of the excitation pole and $A_g$ is the cross sectional area of the excitation pole. Also,

$$R_{pm} = \frac{1}{P_{m0}} + R_g \tag{6}$$

is the reluctance of the PM poles and

$$R_s = \frac{l_s}{\mu_0 A_s} \tag{7}$$

is the reluctance of the dot between two poles, where

$l_s$ the slot depth plus the air gap length,
$A_s$ the section area of the slot
$F_{ex}$ the MMP of the field winding of excitation pole, assuming that the 2 poles have the same MMF value but in opposite direction.
$F_{ex}$ the MMP produced by field winding.

The circuit is described by the following equation:

$$\sum_{i=1}^{12} \frac{1}{R_i} \cdot P = \sum_{i=1}^{12} \frac{F_i}{R_i} \tag{8}$$

where

$P$ the magnetic potential of the rotor core (taking stator core as zero reference),
$F_i$ the MMF of branch $i$,
$R_i$ the reluctance of the branch $i$,

Since the magnets and field windings are present in pairs and thus cancel each other, $\sum_{i=1}^{12} \frac{F_i}{R_i}$ is always zero.

Solving equation (8) yields

$$P = 0 \tag{9}$$

Thus the flux of a branch $i$ is

$$\Phi_i = \frac{1}{R_i} \cdot F_i \tag{10}$$

So, the flux of an excitation pole is

$$\Phi_{ex} = \frac{F_{ex}}{R_g} \tag{11}$$

and the flux of a PM pole is

$$\Phi_{pm} = \frac{F_{pm}}{R_{pm}} \tag{12}$$

From equation (11) it is apparent that changing $F_{ex}$ can easily change the flux of the excitation poles, since the air gap reluctance $R_g$ is normally very small. However, the flux of the PM

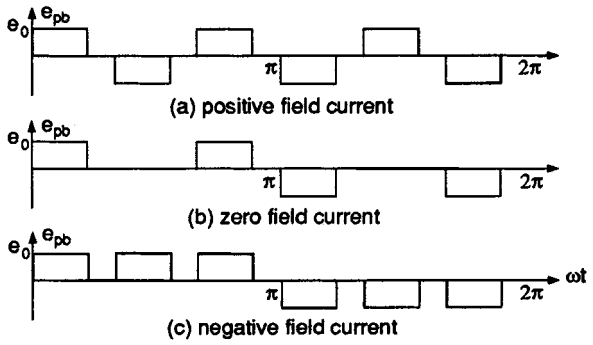


Fig. 4. Back EMF of a phase belt winding.

pole is difficult to change due to the typically large value of reluctance $R_{pm}$.

The armature winding of SynPM machines should be connected in the way that when field current changes, it can change the back EMF of a circuit, assuming that speed is maintained constant.

*2) Back EMF of a Phase Belt Winding:* The induced voltage (EMF) of a phase belt winding is

$$e_i = \frac{d\Lambda_i}{dt} \tag{13}$$

Each phase belt winding will encounter a PM pole, a second PM pole, then an excitation pole as the rotor rotates. Since the flux of the excitation pole is adjustable, the back EMP of a phase belt winding has the waveform shown in Fig. 4. Fig. 4(a) show the "field strengthening" case when the field current has the value such that the excitation pole flux magnitude is the same as the PM pole flux. Fig. 4(b) shows the "field weakening" case when the field current is zero. Fig. 4(c) shows the "demagnetizing" case when the field current is in the opposite direction.

Having realized the phase belt winding back EMF as shown in Fig. 4, a circuit can now be formed by connecting three consecutive phase belt windings of the same phase in series, so that at any moment the circuit is always under the influence of one excitation pole and 2 PM poles, resulting in an adjustable circuit back EMF. Fig. 1 shows the required circuit connection. The resulting back EMF's of the circuit for the cases of positive field current, no field current and negative field current are shown in Figs. 5, 6, and 7.

Three special cases are interesting to study. Assume that at a certain speed the magnitude of the back EMF induced by the PM pole flux in a phase belt winding is $e_0$. As the first case assume that a certain positive excitation is applied such that the flux produced by excitation pole is the same as that of a PM pole and in the opposite direction of its neighboring PM poles. In this case the back EMF of the circuit is

$$e_{cir} = 3 * e_0 \tag{14}$$

as shown in Fig. 5.

The second cue occurs when the field current is zero. The back EMF of the circuit is

$$e_{cir} = 2 * e_0 \tag{15}$$

as shown in Fig. 6.

A third case exists when a certain negative excitation is applied such that the flux produced by the excitation pole is the same as that of a PM pate and in the same direction of its neighboring PM poles. In this case the back EMF of the circuit is

$$e_{cir} = 2 * e_0 - e_0 = e_0 \tag{16}$$

as shown in Fig. 7.

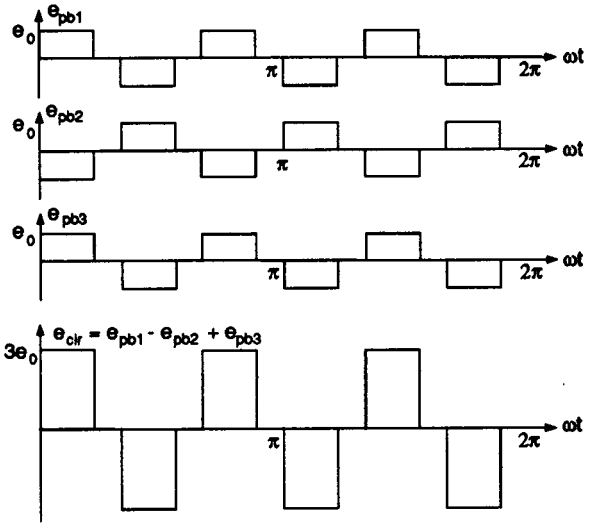


Fig. 5. Back EMF of one circuit with full positive excitation.

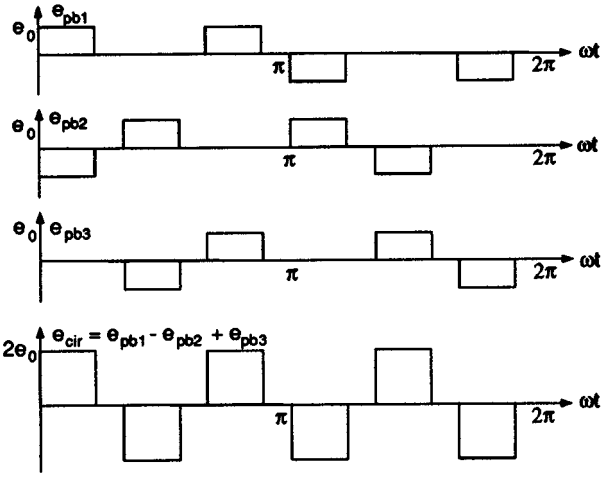


Fig. 6. Back EMF of one circuit with zero excitation.

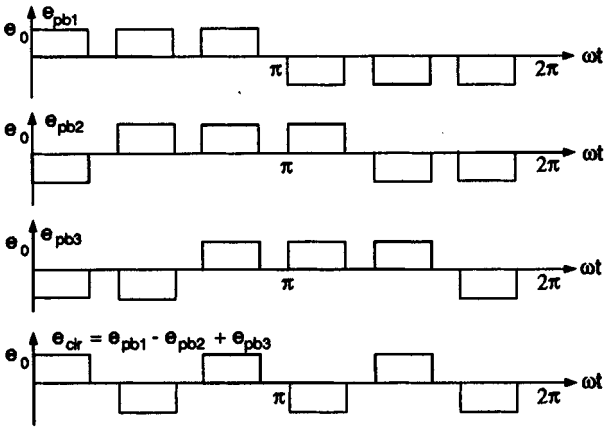


Fig. 7. Back EMF of one circuit with full negative excitation.

If the machine has a sinusoidal back EMF, then

$$e_{cir} = 2\omega\Lambda_{pm} + \omega\Lambda_{ex} \tag{17}$$

Because $\Lambda_{ex} = L_f i_f$, circuit back EMF can also be written as

$$e_{cir} = 2\omega\Lambda_{pm} + \omega L_f i_f \tag{18}$$

which shows that $e_{cir}$ is regulated by $i_f$. However, it should be noted that the flux density under the PM poles remains almost unchanged.

## III. Circuit Model

From the structural features of the SynPM machine, it is evident that the new machine is a combination of a PM machine and a synchronous machine. There are two major features that make SynPM machines distinct from both synchronous and PM machines. One advantage is that SynPM machines have adjustable air gap flux density compared with the PM machine. The other is that the armature reaction inductance of SynPM machine is lower than synchronous machine and higher than normal PM machine placing it in a desirable range for the purpose of controlling terminal voltage.

### A. Steady State Model

The voltage equation for a synchronous machine and PM machine with a sinusoidal waveform is

$$V = I \cdot R + jI_d x_d + jI_q x_q + E \tag{19}$$

The power equation is

$$P = \frac{EV}{x_d} sin(\gamma) + V^2 sin(2\gamma)(\frac{1}{x_q} - \frac{1}{x_d}) \tag{20}$$

where $\gamma$ is the angle between phasors $E$ and $V$. It can be noted that there is no difference between synchronous machine and PM machine. Only the sources of the flux are different.

Having obtained equation (19), a phasor diagram can be used to show the field weakening case. In this phasor analysis, the voltage is kept constant. Since the back EMP can be controlled by the field current, the armature current vector is assumed to be perpendicular to the field flux. i e., only $q$ axis current is present.

It is assumed that for field weakening operation, the current and voltage are limited by the converter rating. i.e., $I_q$ and $V$ are constant. Since the current is assumed to have only a $q$ axis component, the voltage equation is

$$V = E + jI_q\omega L_q \tag{21}$$

and the corresponding phasor diagram is shown in Fig. 8.

Since $V$ is constant and $j\omega I_q$ is perpendicular to $E$, the locus forms a circle:

$$V^2 = E^2 + (I_q\omega L_q)^2 \tag{22}$$

Dividing equation (22) by $\omega^2$, one obtains

$$(\frac{V}{\omega})^2 = \Lambda^2 + (I_q L_q)^2 \tag{23}$$

Assuming that the rated speed is $\omega_0$, the maximum speed for keeping the current aligned with the Q-axis and constant is $\omega_{max}$, and the minimum flux linkage is $1/k$ of that of rated value, then at the rated speed

$$(\frac{V}{\omega_0})^2 = \Lambda_0^2 + (I_q L_q)^2 \tag{24}$$

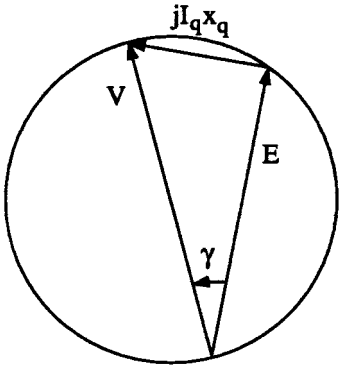


Fig. 8. Circle of voltage equation neglecting resistance.

and at the maximum speed

$$(\frac{V}{\omega_{max}})^2 = (\frac{\Lambda_0}{k})^2 + (I_q L_q)^2 \tag{25}$$

After some algebra the relation between maximum speed $\omega_{max}$ and rated speed $\omega_0$ is

$$\omega_{max} = \frac{k\omega_0}{\sqrt{1 + (k^2 - 1)(\frac{I_q x_q}{V})^2}} \tag{26}$$

where $x_q = \omega_0 L_q$ is the Q-axis reactance at rated speed $\omega_0$. If $\frac{I_q x_q}{V} = 0.3$ and $k = 3$, then the speed range under this condition is about 2.29 for the ideal case. This result indicates that the speed range will not exceed 3 and to gain a wider range, a smaller $x_q$ is desirable.

### B. Transient Model

One can also expect, the transient model of SynPM machine to be the combination of the transient models of the synchronous and PM machines, as expressed in the following equations, assuming a laminated rotor without damping winding:

$$\begin{bmatrix} v_q \\ v_d \\ v_0 \\ v_f \end{bmatrix} = \begin{bmatrix} r_a & 0 & 0 & 0 \\ 0 & r_a & 0 & 0 \\ 0 & 0 & r_a & 0 \\ 0 & 0 & 0 & r_f \end{bmatrix} \begin{bmatrix} i_q \\ i_d \\ i_0 \\ i_f \end{bmatrix} + \begin{bmatrix} \frac{d\Lambda_q}{dt} \\ \frac{d\Lambda_d}{dt} \\ \frac{d\Lambda_0}{dt} \\ \frac{d\Lambda_f}{dt} \end{bmatrix} \tag{27}$$

and

$$\begin{bmatrix} \Lambda_q \\ \Lambda_d \\ \Lambda_0 \\ \Lambda_f \end{bmatrix} = \begin{bmatrix} L_q & 0 & 0 & 0 \\ 0 & L_d & 0 & L_{df} \\ 0 & 0 & L_0 & 0 \\ 0 & L_{fd} & 0 & L_{ff} \end{bmatrix} \begin{bmatrix} i_q \\ i_d \\ i_0 \\ i_f \end{bmatrix} + \begin{bmatrix} 0 \\ \Lambda_{pm} \\ 0 \\ 0 \end{bmatrix} \tag{28}$$

## IV. Coupled Circuit Simulation

The $d-q$ model of an AC machine is well established and widely used in analysis of AC drives. It is based on the assumption that the stator wings and air gap flux density are sinusoidally distributed. However, this assumption is far from reality in some cases, such as the newly emerging doubly salient PM machine [5], or an induction or synchronous reluctance machine un der fault conditions (one phase short/open circuit, etc.) A model based on the basic geometry and winding layout of an

arbitrary $n$ phase machine would be much more suitable for a general purpose, time domain simulation of the SynPM machine in the coupled circuit model the parameters such as mutual inductance and the PM induced flux linkages are considered to be time-varying and can be evaluated in real time, white secondary parameters such as end-turn effect, leakage inductances are treated as constants. The model has been successfully used in the analysis of induction and synchronous reluctance machines [6] [7].

The circuit equations of a SynPM can be written as

$$V_s = R_s I_s + \frac{d\Lambda_s}{dt} \tag{29}$$

$$V_r = R_r I_r + \frac{d\Lambda_r}{dt} \tag{30}$$

$$\Lambda_s = L_{ss} I_s + L_{sr} I_r + \Lambda_{spm} \tag{31}$$

$$\Lambda_r = L_{rs} I_s + L_{rr} I_r + \Lambda_{rpm} \tag{32}$$

where

| | |
|---|---|
| $R_s$ | diagonal matrix of stator resistances, |
| $R_r$ | diagonal matrix of rotor resistances, |
| $L_{ss}$ | stator inductance matrix, |
| $L_{rr}$ | rotor inductance matrix, |
| $L_{sr}$ | stator to rotor mutual inductance matrix, |
| $L_{rs} = L_{sr}^T$ | rotor to stator mutual inductance matrix, |
| $I_s$ | stator current vector, |
| $I_r$ | current vector |
| $V_s$ | stator voltage vector, |
| $V_r$ | rotor voltage vector, |
| $\Lambda_{spm}$ | the flux linkage produced solely by magnets and coupled with stator windings, |
| $\Lambda_{rpm}$ | the flux linkage produced solely by magnets and coupled with rotor windings. The torque is |

$$T_{em} = \frac{1}{2} I_s^T \frac{dL_{ss}}{d\theta} I_s + I_s^T \frac{dL_{sr}}{d\theta} I_r + I_s^T \frac{d\Lambda_{pms}}{d\theta} \tag{33}$$

The mechanical equations are

$$\frac{d\omega}{dt} = \frac{1}{J}(T_{em} - T_{load}) \tag{34}$$

$$\frac{d\theta}{dt} = \omega \tag{35}$$

where

| | |
|---|---|
| $\theta$ | the mechanical angle, |
| $\omega$ | mechanical speed, |
| $T_{load}$ | load torque, |
| $J$ | the inertia of the rotor and load |

In summary, equations (29), (30), (31), (32), (33), (34) and (35) form the mathematical model for a general electric machine and also form basis for the mathematical model for SynPM machine simulation.

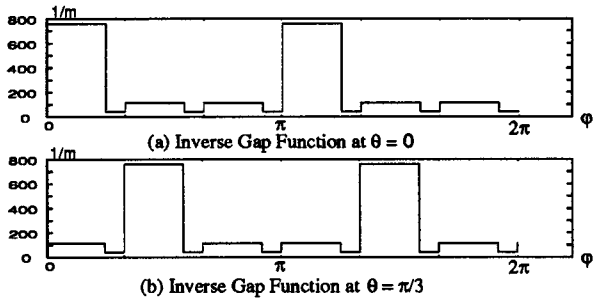


Fig. 9. Inverse gap function at $\theta = 0$ and $\theta = \frac{\pi}{3}$.

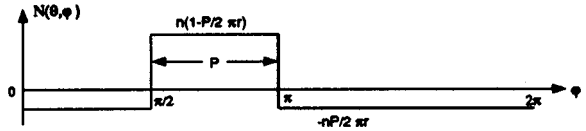


Fig. 10. Winding function of a full pitch coil for a 4 pole machine.

### A. Calculation of Inductances

It is apparent that the calculation of all the machine inductances as defined by the inductance matrices in the previous section is the key to the successful simulation of the machine. There are many methods to calculate the inductances of an electric machine such as finite elements and the magnetic circuit method. However, the winding function method is a convenient means for calculating inductances if the bulk of iron in both stator and rotor are assumed to have infinite permeance. This method assumes no symmetry in the placement of any electric machine coils in the slots. According to winding function theory, the mutual inductance between any two windings $i$ and $j$ in any electric machine can be computed by the following equation [8]:

$$L_{ij}(\theta) = \mu_0 L r \int_0^{2\pi} g^{-1}(\theta, \varphi) N_i(\theta, \varphi) N_j(\theta, \varphi) d\varphi \tag{36}$$

where

| | |
|---|---|
| $\theta$ | the angular position of the rotor with respect to a stator reference, |
| $\varphi$ | a particular angular position along the stator inner surface, |
| $g^{-1}(\theta, \varphi)$ | the inverse gap function which is the inverse of the air gap versus the angular positions $\theta$ and $\varphi$, |
| $L$ | the length of stack, |
| $r$ | the average radius of air gap. |

The term $N_i(\theta, \varphi)$ is called the winding function and represents, in effect, the MMF distribution along the air gap for a unit (one ampere) current flowing in winding $i$. An example of the inverse gap function is shown in Fig. 9. Fig. 10 shows winding function of a coil at a certain rotor position $\theta$.

The calculated coil inductance versus rotor angular position curves are shown in Fig. 11(a), (b), and (c). From the curve one can observe that there are two angular positions where the coil self inductance reaches its maximum value. This result reflects the fact that there are two excitation poles and under these two poles the coils see a flux path with the least reluctance.

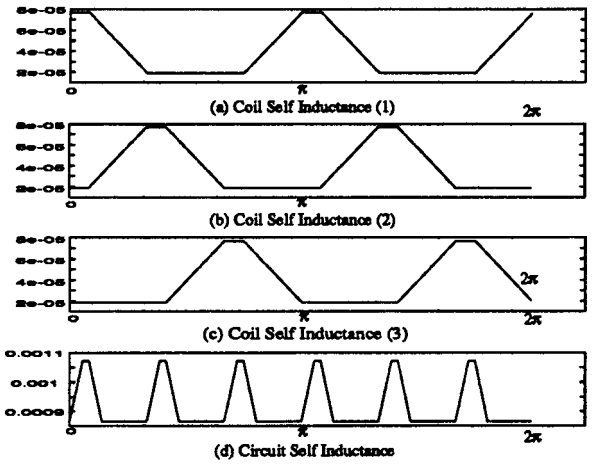


Fig. 11. Calculated coil and circuit inductances.

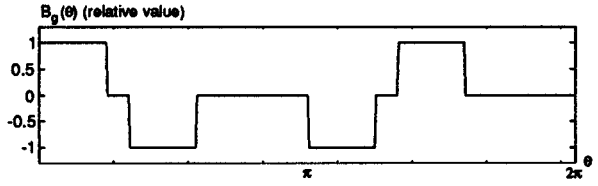


Fig. 12. Air gap flux density produced by PM.

Fig. 11(d) shows the calculated circuit self inductance versus rotor angular position curve. There are six positions where the inductance reaches its maximum as a result of the series connection of the member coils of the circuit.

### *B. Calculation of Flux Linkages Produced by PM*

The flux linkage of circuits produced by PM poles is another important issue in the simulation. Having the magnetic model and the assumptions made previously, it is not hard to calculate the air gap flux density distribution. Fig. 12 shows the calculated air gap flux density distribution.

After the air gap flux density under the PM pole is calculated, the flux density in air gap produced by magnets can be drawn. The flux linkage of a coil is determined by the integral

$$\Lambda_c = nrl \int_{\theta_1}^{\theta_2} B_g(\theta) d\theta \tag{37}$$

where $B_g(\theta)$ is the PM caused flux density, $\theta_1$ is the angular position of the first coil side, $\theta_2$ is the angular position of the second coil side, $n$ is the number of turns of the coil, $r$ is the average air gap radius, and $l$ is the effective stack length.

Fig. 13(a), (b), and (c) show the calculated flux linkage of a coil versus rotor angular position curve. In the curves it can be seen that there are four rotor angular positions where the flux linkage reaches its maximum magnitude which corresponds to the fact that the SynPM machine has four PM poles.

The circuit flux linkage is the sum of the flux linkages of all of its member coils. That is,

$$\Lambda_{ckt} = \sum_{i=1}^{i=m} \pm \Lambda_c \tag{38}$$

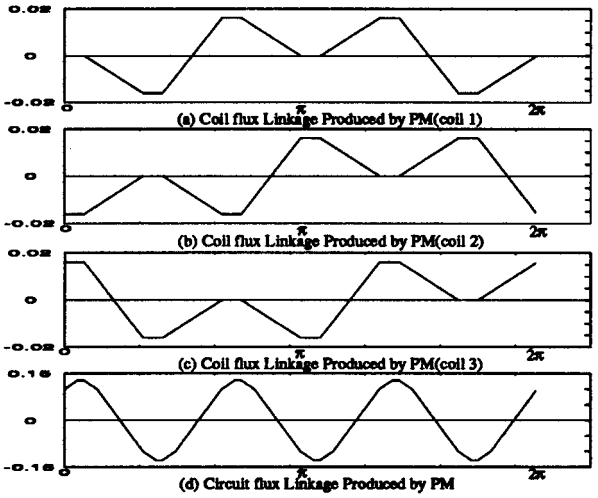


Fig. 13. Calculated flux linkages of coils and circuit.

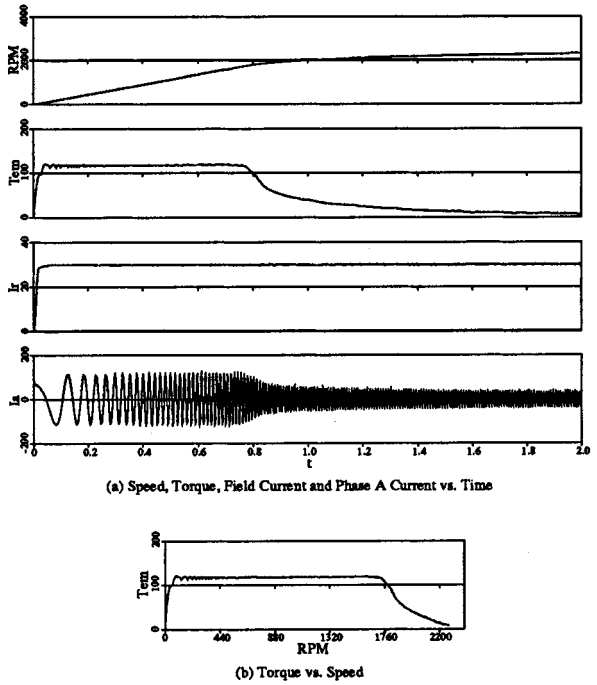


Fig. 14. Simulation of SynPM machine, without field current regulation.

where $m$ is number of coils in the circuit. The sign before $\Lambda_c$ is determined by the manner in which the coil is connected to form the circuit.

A curve of the circuit flux linkage versus rotor angular position is shown in Fig. 13(d). From the curve it is clear that from the terminals of the circuit, the number of poles is six, which is achieved by connecting the coils of same phase under all poles in series.

### *C. Simulation*

A simulation study has been made to determine the performance of the SynPM machine using the circuit equations that have been derived. All of the rotor dependent parameters such as the inductances and derivative of inductances are "looked up" according to the rotor position as previously mentioned. The simulation results are shown in Figs. 14 and 15. From these

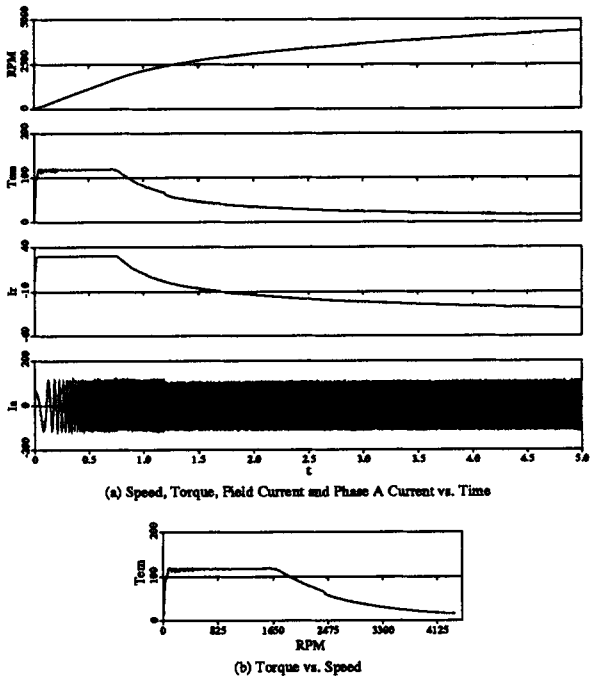


Fig. 15. Simulation of SynPM machine with field current regulation.

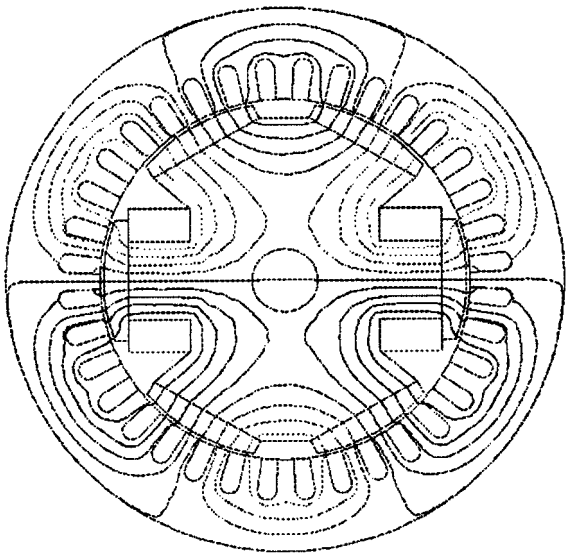

Fig. 16. Flux lines of a 6 pole SynPM machine with full positive field current.

plots, it should be clear that the SynPM machine with field current regulation capability has much higher constant power speed range with considerably improved torque capability than an equivalent PM machine. In these computer traces current regulated pulse width modulation was used to control the stator and rotor current. The field weakening range has been extended from 1.3 to 2.7 per unit or greater compared to a machine without current regulation.

## V. Finite Element Analysis

To verify the results of the ideal magnetic circuit analysis, a FEM analysis was also conducted. The FEM analysis package used is ANSOFT's Maxwell 2D model. Fig. 16 shows the flux

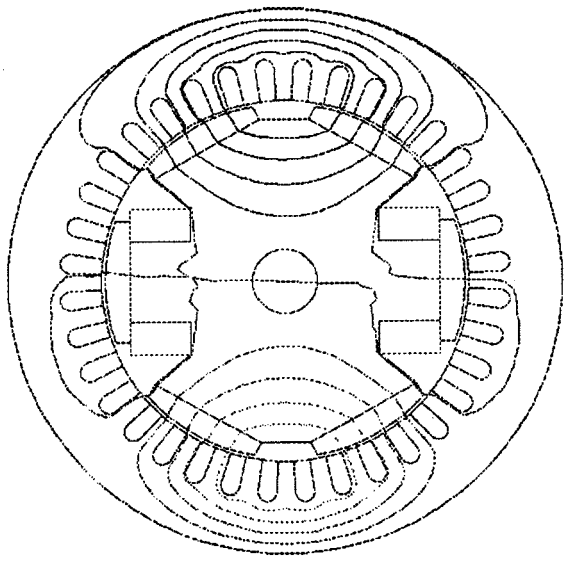

Fig. 17. Flux lines of a 6 pole SynPM machine with zero field current.

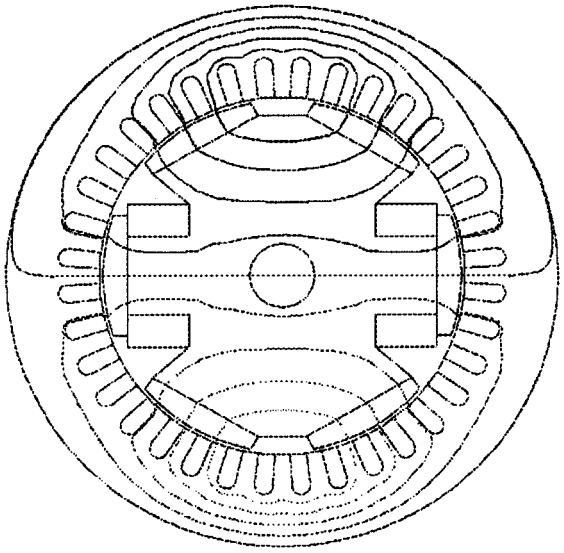

Fig. 18. Flux lines of a 6 pole SynPM machine with full negative field current.

lines of the SynPM machine with positive field current, i.e., the field strengthening case. Fig. 17 shows another case of the SynPM machine with zero field current, and, finally, Fig. 18 shows the case where the field current is negative, or the field weakening case. From these FEM resulting plots it is apparent that a change of field current does indeed change the flux pattern in the SynPM machine as predicted.

## VI. Conclusion

A new synchronous/permanent magnet hybrid machine has been presented in this paper and its working principle has been demonstrated. It can work as a generator or a motor. Although 6 pole version is discussed here, an 8 pole version functions in a similar manner with 4 PM poles and 4 excitation poles.

The SynPM machine has true field regulation capability. The machine can operate at high speed with field weakening capability. It has potentials of achieving high efficiency and high

power density due to the use of PM material. The ability to operate as pure PM machine increases its reliability. However, the slip ring and brushes are still present. There is high flux density present in the stator core region between two adjacent PM poles at high speed when weakening the field, which may cause high iron loss in the stator core.

Considering the gains in power density, efficiency and reliability, it can be concluded that the SynPM drive has potential to compete with conventional AC induction motor drives in higher horsepower applications where the added cost of the rotor structure is offset by the improvement gains in size and weight of the machine and by reduced cost in the power converter. However, combining 4 pole or 2 pole field flux at field weakening with the 6 pole flux of the armature reaction will result in a number of space and time harmonic components. This could generate undesirable torque pulsations and vibration. A thorough assessment of this problem requires an extensive analysis and is clearly outside the space allotment for this paper. This problem should form the nucleus for future work on this new machine.

## REFERENCES

[1] T. A. Lipo, "Recent Progress in the Developmcnt of Solid-State AC Motor Drives," *IEEE Trans. Power Electronics*, vol. 3, no. 2, pp. 105–117, April 1988.

[2] B. K. Bose, "Power Electronics and Motion Control—Technology Status and Recent Trends," *IEEE Trans. Ind. Applic.*, vol. IA-29, no. 5, pp. 902–909, Sep/Oct 1993.

[3] T. J. E. Miller, *Brushless Permanent-Magnet and Reluctance Motor Drives*. Oxford: Clarendon Press, 1989.

[4] T. A. Lipo, "Synchronous Reluctance Motor—A Viable Alternative for Adjustable Speed Drive?," *Electrical Machines and Power Systems*, vol. 19, no. 6, pp. 659–671, Sept. 1991.

[5] Y. Liao, F. Liang, and T. A. Lipo, "A Novel Permanent Magnet Motor with Doubly Salient Structure," in *IEEE Industry Applications Soc. Conf. Rec.*, vol. 1, 1992, pp. 308–316.

[6] X. Luo, Y. Liao, H. Toliyat, A. El-Antably, and T. A. Lipo, "Multiple Coupled Circuit Modeling of Induction Machines," *IEEE Trans. Ind. Applic.*, vol. IA-31, no. 2, pp. 311–318, March/April 1995.

[7] X. Luo, A. El-Antably, and T. A. Lipo, "Multiple Coupled Circuit Modeling of Synchronous Reluctance Machines," in *IEEE Industry Applications Soc. Conf. Rec.*, vol. 1, 1994, pp. 281–289.

[8] T. A. Lipo, "Theory and Control of Synchronous Machines," ECE Department, University of Wisconsin-Madison, Course Notes for ECE 5ll, 1995.